Energy, Mines and Resources Canada
Énergie, Mines et Ressources Canada

CANMET

Canada Centre for Mineral and Energy Technology
Centre canadien de la technologie des minéraux et de l'énergie

CONVERSION OF NON-COKING COALS TO COKING COALS BY THERMAL HYDROGENATION

B.N. Nandi, M. Ternan and K. Belinko

JANUARY 1980

For submission to fuel

ENERGY RESEARCH PROGRAM
ENERGY RESEARCH LABORATORIES
REPORT ERP/ERL 80-8(J)

CONVERSION OF NON-COKING COALS TO COKING COALS BY THERMAL HYDROGENATION

by

Biswanath, N. Nandi, Marten Ternan and Keith Belinko
Energy Research Laboratories
Department of Energy, Mines and Resources
Ottawa, Ontario, K1A 0G1, Canada

SUMMARY

Coking properties were observed in four non-coking coals, a lignite, a sub-bituminous coal, a semi-anthracite and an oxidized bituminous coal which had been treated by partial thermal hydrogenation. The effects of temperature, reaction time and hydrogen pressure on liquid and solid product yields were examined. Microscopic examination of the hydrogenated solid residues showed that they all contained anisotropic structures somewhat spherical in shape which are associated with mesophase development.

The dilatation, plastic character and free swelling index of the hydrogenated solid products were considerably better than those of the original coals. Dilatation residues produced from hydrogenated solids exhibited anisotropic structures.

SHORT STATEMENTS

(1) Principal New Conclusions and Results

Microscopic evidence is presented for the formation of spherical structures (mesophase) during the development of coking properties in non-coking coals. Solid and liquid yields resulting from the thermal hydrogenation of non-coking coals are presented. The differences in behavior of non-coking coals of varying rank during thermal hydrogenation are compared.

(2) Methods and Observations

Standard experimental procedures were used.

(3) Special Limitations and Assumptions

None.

INTRODUCTION

For the past few years, research in our laboratories has been directed toward the production of distillate liquid fuels by high pressure hydrogenation of residual oils and coals. In the course of this program hydrogenated coal residues were found to have microstructures resembling those of metallurgical coke (1), even though the coal originally used was not a coking coal. Subsequently, additional experiments were performed to confirm this observation. The purpose of the present paper is to compare our preliminary findings (2,3) with more extensive data. Results are reported which demonstrate the development of coking properties in a semi-anthracite non-coking coal, a sub-bituminous non-coking coal, a lignite, and a coking coal whose coking properties had been destroyed by oxidation.

The development of coking properties in non-coking coals was first reported by King and co-workers (4,5,6). Orchin et al (7) found that high pressure hydrogenation would restore the coking properties of a coal whose coking properties had been destroyed by oxidation. Ahuja et al (8,9) used a non-coking coal having a high oxygen content to study the effects of temperature and hydrogen pressure on the development of coking properties. Kukharenko and Matveeva (10) also found that hydrogenation improved the coking properties of non-coking coals.

Experiments described here were performed as a function of hydrogen pressure, temperature and residence time in order to determine the effects of processing conditions on the development of coking properties. Although high pressure hydrogenation produced the same effect (the development of coking properties) in all of the coals studied, it was recognized that different reactions occurred in each of the different types of materials. The results have been related to recent concepts (11,12).

EXPERIMENTAL PROCEDURE

Hydrogenation of the various non-coking coals whose properties are listed in Tables 1 and 2 was carried out in a stainless steel, vertical fixed bed reactor of 155 mL capacity (13). In the first series of experiments (Table 3) approximately 50-100 g of coal particles having

dimensions of 2.38 - 4.76 mm, were introduced into the reactor, and electrolytic hydrogen (99.9% purity) was passed up through the bed at 2.8 L/min at S.T.P. The vapour phase material leaving the reactor flowed to a high pressure receiver vessel where condensation occurred. The liquid product accumulated in the bottom of the receiver vessel for the duration of the experiment. The gases flowed continuously out of the top of the receiver vessel. The pressure within the reactor was maintained at 13.9 MPa. The gas flow was initiated at the same time as the heating cycle. The temperature of the reactor was raised to 450°C over a period of one hour and held constant at that temperature for 3 h. At the end of the experiment, the reaction bed was allowed to cool in a hydrogen atmosphere. In some of the experiments, (Table 4) nitrogen gas was used instead of hydrogen to confirm that the results obtained were in fact associated with hydrogenation of the coal rather than with high pressure effects.

In subsequent experiments, the effect of reactor temperature, reactor pressure and residence time were investigated during hydrogenation of a sub-bituminous coal (Forestburg) and an oxidized bituminous coal (Phalen Seam). Temperatures, pressures and reaction times ranging from 375°C to 475°C, 0.79 MPa to 20.8 MPa and 0-10 hours were studied.

The material removed from the reactor subsequent to hydrogenation generally showed some degree of agglomeration along with the presence of a pitch-like material. The liquid and solid yield were recorded for each experiment. The liquid yield was the amount of material accumulated in the receiver vessel. The solid yield was the amount of material remaining in the reactor at the conclusion of the experiment. For most of the hydrogenated products, thermal rheological properties such as Free Swelling Index (FSI) (according to ASTM specification D720) and dilatation were determined and proximate and ultimate analyses were carried out. Oxygen content of some of the samples was determined using a Perkin-Elmer (Model 240) Elemental Analyser. Dilatation tests were performed in a Ruhr Dilatometer at a heating rate of 3°C/min to 550°C, according to German Specification DIN 51 739.

Microscopic examinations of the various samples were performed with a Leitz Reflected Light Microscope. The samples were embedded in Lucite plastic and polished according to ASTM specifications. Micrographs were taken at a magnification of 600 times, using partially crossed nicols.

RESULTS AND DISCUSSION

Proximate analyses of the various non-coking coals used in the present work are given in Table 1. Dilatometer residues of these coals at 550°C, resulted in non-agglomerated chars. Dilatation results and FSI's for these coals are given in Table 2 and reflect their non-coking characters. The dilatation residue obtained from experiments with original Onakawana lignite did not show any coke structure (Figure 1). Similar isotropic structures were observed for the other original three non-coking coals studied.

The four coals listed in Table 1 were hydrogenated for 3.0 h at 450°C and a hydrogen pressure of 13.9 MPa. FSI and dilatation results for the hydrogenaged residues, given in Table 3, were found to improve considerably over those of the original coals. The dilatation residues were found to be agglomerated and hard. The results clearly show that thermal hydrogenation enhances coke formation in non-coking coals.

No single mechanism to explain coke formation has yet attained universal acceptance. However, the mechanism by which coke is formed from nematic liquid crystals (11,12) is accepted for many situations.

The above mechanism is known to be valid when the carbonaceous starting material is petroleum pitch, coal tar, coal derived liquid or certain pure compounds. The formation of anisotropic spheres (mesophase) during the carbonization of these materials is extensively documented in the literature (11,12).

The role of spheroidal structures (mesophase) during the formation of coke from coal has not been readily observed. Patrick, Reynolds and Shaw (14,15) were unable to find any spherical structures (mesophase) during the carbonization of British Coals. Marsh et al (16) reported the existence of fused spheres in only two of the fourteen American coals they investigated although they did not present any optical microscopic results. Goodarzi and Murchison (17) have commented on the uncertainty of spheriodal structure (mesophase) formation from coals. Marsh and Walker (18) have categorically stated that coal substances do not form spherical units.

Evidence for the formation of mesophase spherical structures from non-coking coals during thermal hydrogenation is shown in Figures 2-5.

Spheres are readily apparent in Figure 2 (hydrogenated lignite), Figure 3 (hydrogenated sub-bituminous coal) and in Figure 4 (hydrogenated coking coal which had been oxidized). In contrast the hydrogenated semi-anthracite in Figure 5 has a flow-type structure. When the hydrogenated agglomerated residues were carbonized during the dilatation tests coke structures similar to those typical of coking coals were obtained. The coke structures are shown in Figures 6-8. The dilatation residue obtained from experiments with hydrogenated semi-anthracite was found to have the same structure as that of the hydrogenated residue (Figure 5) suggesting that it had been partially converted to coke during the hydrogenation experiment. This was further confirmed by the lack of contraction or dilatation in the case of hydrogenated residue from semi-anthracite (Table 3).

In principle, the improved coking properties of the hydrogenated residues shown in Table 3, compared to the original coals shown in Table 2, could be caused either by the high mechanical pressure or by the chemical influence of the hydrogen. The data in Table 4 show that coking properties did not develop when high pressure nitrogen was used instead of high pressure hydrogen. The microstructure of the solids obtained from the high pressure nitrogen experiments was the same as the original coal, that is similar to the structure shown in Figure 1. This demonstrated the necessity for the chemical influence of hydrogen.

Other workers who placed their samples in closed containers have claimed that high pressures alone enhanced coke formation. Huttinger and Rosenblatt (19) put their samples in covered porcelain crucibles. Goodarzi et al (20) and Walker and co-workers (21,22) put their samples into sealed nobel-metal tubes. One can speculate on mechanisms which would reconcile the results of these workers (19-22) and our own. The vapourized tar and gases produced upon heating would remain with the coal when sealed containers are used. Polymerization of this tar could assist mesophase formation (23) and act as a binder. Sealed containers would also retain hydrogen, methane and other gases evolved from the coal. These evolved gases may have performed the same function as hydrogen in our experiments. With the flow system used for our nitrogen experiments all of these materials (vapourized tar, hydrogen etc.) would be swept out of the reactor.

The effects of processing conditions are shown in Tables 5 to 8 and in Figures 9,10 and 11. As the hydrogen pressure increased, the coking

tendencies of the hydrogenated residues also increased (Tables 5 and 8). These results are in accord with those reported by Ahuja et al (8,9). Figure 9 very clearly shows a decrease in the yield of solid hydrogenated product. The yield data for the liquid although scattered badly do support an increase in liquid product yield with increasing hydrogen pressure. The combined data indicate that at higher hydrogen pressures there is a greater conversion of coal to gaseous and liquid products. Furthermore, the development of coking properties in the hydrogenated solid residue is enhanced at higher pressures.

The hydrogenation pressure was found to have a profound influence on the microstructure of the solid. This is demonstrated, for example, in Figures 12-15 for various reactor hydrogen pressures. The dilatation residue from the hydrogenated coal obtained at 13.9 MPa was found to have a predominantly flow-type structure, whereas the dilatation residues of the products from experiments at lower hydrogen pressures were found to have coarse (Figure 13) and fine grain (Figure 14) mosaic coke structures. The size of the mosaic grain was found to decrease with decreasing hydrogen pressure during hydrogenation, ultimately resulting in an isotropic coke structure for pressures lower than 3.5 MPa (Figure 15).

It may be that hydrogen at high pressure causes hydrogenation of the free radicals formed on heating (24) and thereby delays polymerization. This concept is supported by the data of Shibaoka and Ueda (25) who concluded that under hydrogen deficient conditions condensation and polymerization occurred. They observed that the mosaic structures became finer as hydrogen became more deficient. Hydrogenation of free radicals will reduce polymerization and probably produce a lower molecular weight residue. Such a residue may provide sufficient fluidity and plasticity to permit molecular re-arrangements (26) leading to the formation of nematic liquid crystals (mesophase).

Variations in coking properties with hydrogen pressure may be caused by diffusion limitations within the coal particles. Alternatively, a large hydrogen chemical potential may be required to permit reaction with the molecular species which constitute coal.

The effects of temperature are shown in Table 6 and in Figure 10. The maximum in liquid yield, minimum in solid yield, and maximum in coking properties all occur within a relatively narrow temperature range. These

optima can be explained in terms of pyrolysis, hydrogenation and polymerization reactions.

As the temperature increases up to 450°C pyrolysis and hydrogenation reactions are responsible for the formation of liquids and tars. The vapourization of these materials causes the increase in liquid and decrease in solid yield shown in Figure 10. At temperatures above 450°C polymerization reactions predominate. When the temperature becomes sufficiently high, hydrogenation becomes thermodynamically less favorable. Eventually the free radicals react with one another (polymerization) more frequently than with hydrogen. These larger molecules remain in the solid phase thereby causing the increase in solid yield and decrease in liquid yield shown in Figure 10.

The coking properties shown in Table 6 follow the same trend. The improvement in coking properties with temperature is consistent with earlier work (8,9). At temperatures above 450°C the dilatation decreases. This is consistent with the occurrence of polymerization reactions and coke formation during the hydrogenation experiments above 450°C.

The effects of reaction time are shown in Table 7 and in Figure 11. The increase in liquid yield and decrease in solid yield with increasing reaction time are consistent. Increasing solid conversion produces more liquid. The interpretation of the coking properties in Table 7 is not as straight forward. The fact that there is a decrease in dilatation at reaction times greater than 3 hours suggests that some polymerized solid product had formed during the hydrogenation treatment. In the previously described high temperature experiments, coke formation by polymerization was associated with a decrease in liquid yield. A decrease in liquid yield with increasing reaction time would be impossible for the experimental results shown in Figure 11. For example, the first three hours of a six hour experiment must be identical to a three hour experiment. It would therefore be impossible for a six hour experiment to produce less liquid than a three hour experiment. This means that the formation of polymerized solid product in this case did not involve the tars present in the vapourized liquids. Instead, coke formation must involve either polymerization of solid species or the formation and subsequent polymerization of some quantity of liquid phase tar species remaining with the solid.

The improvement in coking characteristics of Forestburg and Phalen

Seam coals with increasing hydrogen pressure and reaction time (Tables 5 and 8) was accompanied by decreasing oxygen content (Table 9 and 10) of the hydrogenated residue. The non-coking characteristics of oxidized coking coals have been ascribed to oxygen functional groups (oxygen ether linkages, hydroxyl, carbonyl and carboxyl groups) by Montgomery and co-workers (27,28). Their mechanism is compeltely consistent with the findings in this study. The oxygen content is definitely decreased by hydrogenation as shown in Table 5. Our previous communication (2) noted that infra-red analysis showed an increase in aliphatic $-CH_2$ and $-CH_3$ groups and a decrease in aliphatic -CH groups, aromatic -OH groups, C=O groups, and C-O-C oxygen ether groups, when this coal was hydrogenated. Our experimental observations and those of others (8,9) show conclusively that there is a relationship between the coking properties and the oxygen functional groups. Also, Yang, Sethi and Steinbert (29) reported that a decrease in oxygen ether linkages would explain their results on the conversion of a non-coking coal into a coking coal.

Different phenomena probably occur in each of the coals. In the case of Canmore semi-anthracite coal hydrogenation of aromatics probably ocurred. This could cause increased fluidity which would asist coke formation.

The Phalen Seam bituminous coal is a high fluidity coking coal when it has not been oxidized. The sample used in this study had been naturally oxidized and did not posses coking properties. However, the coal undoubtedly contained all of the components and characteristics required by a coking coal. Thus, the primary effect of hydrogen on this oxidized bituminuous coal was probably to remove the oxygen groups. The data in Tables 8 and 9 certainly show a correlation between the development of coking properties and oxygen removal.

The Forestburg sub-bituminous coal and the Onakawana lignite contain large quantities of oxygen and therefore, also require oxygen removal. During thermal hydrogenation, paraffinic side chains on the coal molecules could also be removed.

The hydrogenation conditions used in these studies are similar to those used in coal liquefaction processes. The work described here suggests that the solid residues from coal hydrogenation processes may have coking properties which would permit blending with other coals for the production of metallurgical coke. If this were true, it would increase the value of the product slate from coal liquefaction processes and therefore improve the financial viability of these projects.

CONCLUSIONS

Thermal partial hydrogenation can develop coking properties in non-coking coals under appropriate conditions. This phenomenon occurs in low rank coals such as lignite and sub-bituminous as well as in high rank coals such as semi-anthracite. Bituminous coals which have lost their coking properties as a result of natural weathering and oxidation can have their coking properties restored by partial hydrogenation. Variations in processing conditions indicated that coking properties improved with increasing hydrogen pressure. At a hydrogen pressure of 13.9 MPa the optimum temperature was approximately 450°C and the optimum reaction time was about 3 hours. The development of coking properties was accompanied by the removal of oxygen functional groups. When the hydrogenation residues were examined with the optical microscope, all of them were found to contain spherical structures associated with mesophase development.

ACKNOWLEDGEMENT

The authors gratefully acknowledge the contributions of I. Johnson, R.J. Williams, S.E. Nixon and B.H. Moffatt for their technical assistance during the course of this work.

REFERENCES

1. Nandi, B.N., Ternan, M., Parsons, B.I., and Montgomery, D.S., Fuel, 1975, 54, 197.

2. Nandi, B.N., Ternan, M., Parsons, B.I., and Montgomery, D.S., 12th Biennial Conference on Carbon, American Carbon Society, 1975, 12, 229.

3. Belinko, K., Ternan, M., and Nandi, B.N., "Chemistry for Energy", Symposium series No. 90 (ed. M. Tomlinson), American Chemical Society, Washington, D.C. 1979, p. 96.

4. Lander, C., Sinnatt, F.S., King, J.G., and Crawford, A., "Improvements in and Relating to the Treatment of Coal and Like Carbonaceous Material", Brit. Pat. Spec, 301720; 1928.

5. Crawford, A., Williams, F.A., King, J.G., and Sinnatt, F.S., "The Action of Hydrogen upon Coal, Fuel Research Technical Paper No. 29", Department of Scientific and Industrial Research, Her Majesty's Stationery Office, London, 1931.

6. Horton, L., King, J.G., and Williams, F.A., Inst. Fuel, December 1933, p. 85.

7. Orchin, M., Golumbic, C., Anderson, J.E., and Storch, H.H., Bulletin 505, U.S. Bureau of Mines, U.S. Government Printing Office, Washington, D.C., 1951, p. 13.

8. Ahuja, L.D., Sharma, J.N., Kini, K.A., and Lahiri, A., J. Sci. Indust. Res, 1958, 17A, 27.

9. Ahuja, L.D., Kini, K.A., Basak, N.G., and Lahiri, A., Proceedings of the Symposium on the Nature of Coal, Central Fuel Research Institute, Jealgora, India, 1959, p. 215.

10. Kukharenko, T.A., and Matveeva, I.I., J. Appl. Chem. of USSR, 1950, 23, 773

11. Brooks, J.D., and Taylor, G.H., "Chemistry and Physics of Carbon", Vol. 4; (ed. P.L. Walker, Jr.), Edward Arnold, New York, 1968, p.243.

12. Marsh, H., and Cornford, C., "Petroleum Derived Carbons", Symposium Series No. 21, (eds. M.L. Deviney and T.M. O'Grady), American Chemical Society, Washington, D.C, 1976, p. 266.

13. Ternan, M., Nandi, B.N., and Parsons, B.I., Mines Branch Research Report R-276, Department of Energy, Mines and Resources, Ottawa, 1974.

14. Patrick, J.W., Reynolds, M.J., and Shaw, F.H., Fuel, 1973, 52, 198.

15. Patrick, J.W., Reynolds, M.J., and Shaw, F.H., Carbon, 1975, 13, 509.

16. Marsh, H., Dachille, F., Iley, M., Walker, P.L., and Whang, P.W., Fuel, 1973, 52, 253.

17. Goodarzi, F., and Murchison, D.G., J. Microscopy, 1977, 109, 159.

18. Marsh, H., and Walker, P.L., Fuel Proc. Technol; 1979, 2, pp. 64,66-67.

19. Huttinger, K.J., and Rosenblatt, V., Carbon, 1977, 15, 69.

20. Goodarzi, F., Hermon, G., Iley, M., and Marsh, H., Fuel, 1975, 54, 105.

21. Hirano, S., Dachille, F., and Walker, P.L., High Temperatures - High Pressures, 1973, 5, 207.

22. Whang, P.W., Dachille, F., and Walker, P.L., High Temperatures - High Pressures; 1974, 6, 127.

23. Makabe, M., Itoh, H., and Ouchi, K., Carbon, 1976, 14, 365.

24. Singer, L.S., and Lewis, I.C., Carbon, 1978, 16, 417.

25. Shibaoka, M., and Ueda, S., Fuel, 1978, 57, 667.

26. Patrick, J.W., Reynolds, M.J., and Shaw, F.H., Fuel, 1979, 58, 501.

27. Wachowska, H.M., Nandi, B.N., and Montgomery, D.S., Fuel, 1974, 53, 212.

28. Ignasiak, B.S., Clugston, D.M., and Montgomery, D.S., Fuel; 1972, 51, 76.

29. Yang, R.T., Sethi, D.S., and Steinberg, M., Fuel, 1978, 57, 315.

CAPTIONS

Figure 1 Optical micrograph of Onakawana lignite carbonized to 550°C, shows characteristic char (C)

Figure 2 Anisotropic spheres (mesophase) in the hydrogenated residue from Onakawana lignite hydrogenated for 3 hours at 450°C and 13.9 MPa. (S-Sphere)

Figure 3 Mesophase formation (M) in the hydrogenated residue from Foresttburg coal hydrogenated for 3 hours at 450°C and 13.9 MPa.

Figure 4 Mesophase formation (M) in hydrogenated residue from oxidized Phalen Seam coal which had been hydrogenated for 3 hours at 450°C and 13.9 MPa.

Figure 5 Flow-type coke structure in Canmore semi-anthracite hydrogenated for 3 hours at 450°C and 13.9 MPa, FS-flow type, UV-unreacted vitrinite.

Figure 6 Optical micrograph of the dilatation residue from hydrogenated Onakawana lignite, CG-coarse grain coke structure.

Figure 7 Optical micrograph of the dilatation residue from hydrogenated Forestburg coal, UV-unreacted vitrinite, F-fusinite

Figure 8 Micrograph of the dilatation residue from the hydrogenated product make from oxidized Phalen Seam coal; OV-oxidized vitrinite, C-coke formation.

Figure 9 Liquid yield (wt %) and Solid yield (wt %) as a function of Hydrogenation pressure (MPa). All experiments were at 450°C for 3 hours. The circles and squares represent Forestburg coal and oxidized Phalen Seam coal respectively.

Figure 10 Liquid yield (wt %) and solid yield (wt %) as a function of temperature (°C). All experiments were at 13.9 MPa for 3 hours. The circles and squares represent Forestburg coal and oxidized Phalen Seam coal respectively.

Figure 11 Liquid yield (wt %) and solid yield (wt %) as a function of reaction time (hours) for Forestburg coal. All experiments were at 450°C and 13.9 MPa.

Figure 12 Dilatation residue of Forestburg coal after hydrogenation at 450°C and 13.9 MPa for 3 hours, showing flow type structure (FS).

Figure 13 Dilatation Residue of Forestburg coal after Hydrogenation at 450°C and 6.9 MPa for 3 hours showing coarse grain structure (CG).

Figure 14 Dilatation Residue of Forestburg coal after hydrogenation at 450°C and 3.5 MPa for 3 hours, showing fine grain structure (FG).

Figure 15 Dilatation residue of forestburg coal after hydrogenation at 450°C and 0.79 MPa for 3 hours, showing initial stages of fine grain structure.

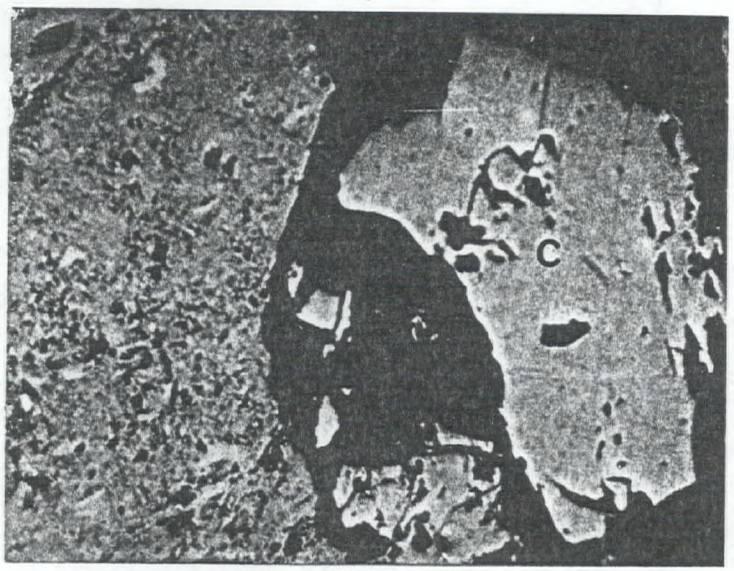

Fig. 1 - Optical micrograph of Onakawana lignite carbonized to 550°C - Shows characteristic char (C).

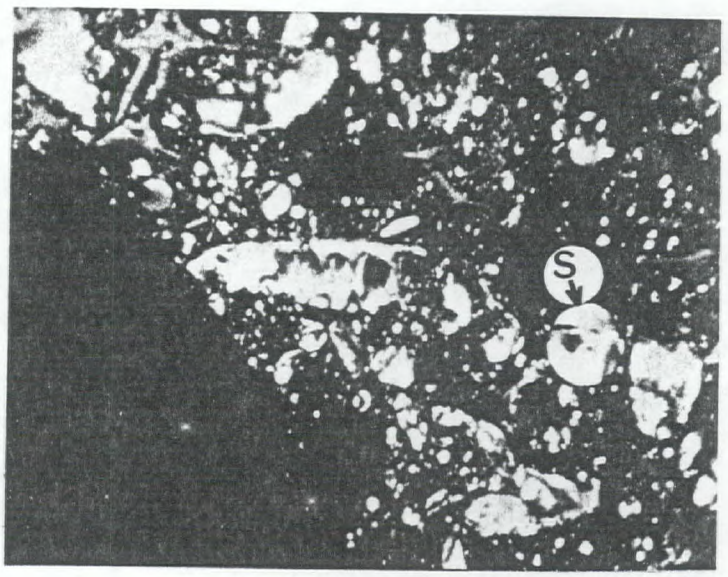

Fig. 2 - Anisotropic spheres (mesophase) in the hydrogenated residue from Onakawana lignite hydrogenated for 3.0 h at 450°C and 13.9 MPa (S - Sphere).

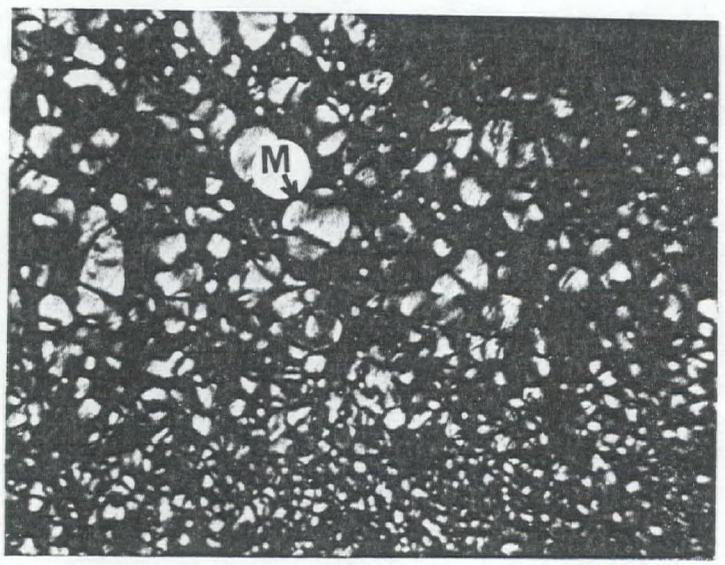

Fig. 3 - Mesophase formation (M) in the hydrogenated residue from Forestburg coal hydrogenated for 3.0 h at 450°C and 13.9 MPa.

Fig. 4 - Mesophase formation (M) in hydrogenated product of oxidized Phalen Seam; 450°C, MPa, 3.0 h.

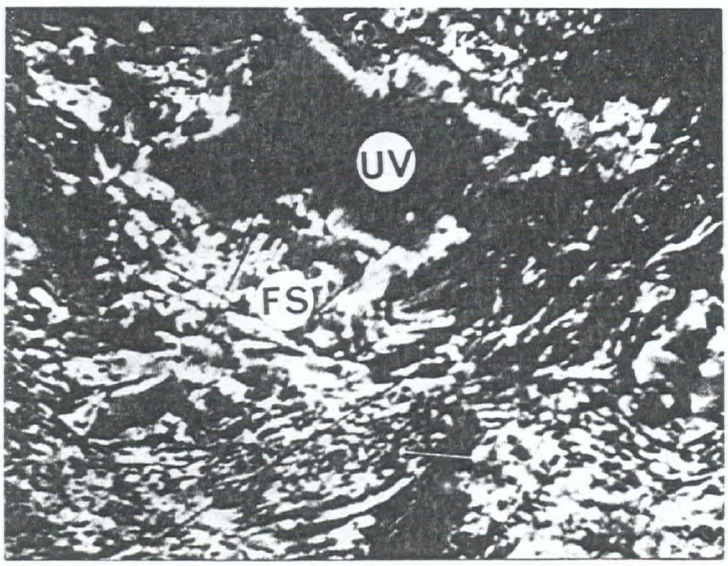

Fig. 5 - Flow-type coke structure in Canmore semi-anthracite hydrogenated for 3.0 h at 450°C and 13.9 MPa, F.S. - flow type, U.V. - unreacted vitrinite.

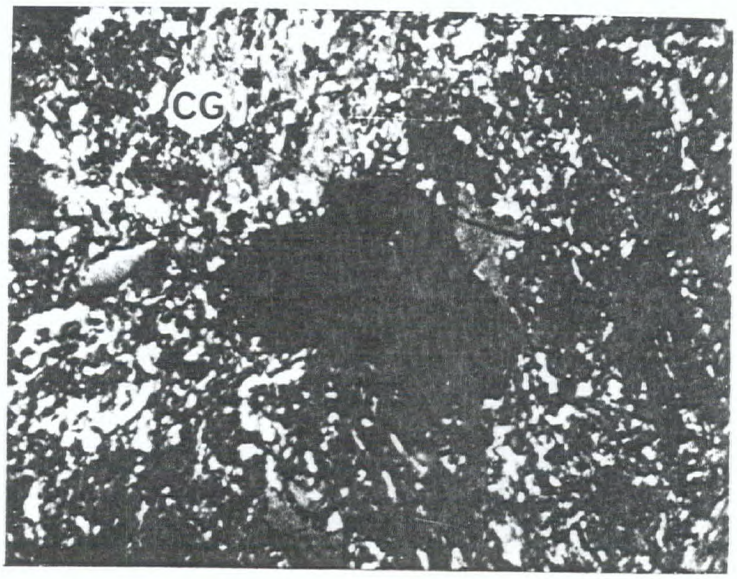

Fig. 6 - Micrograph of the dilatation residue from hydrogenated Onakawana lignite C.G. - Coarse grain coke structure.

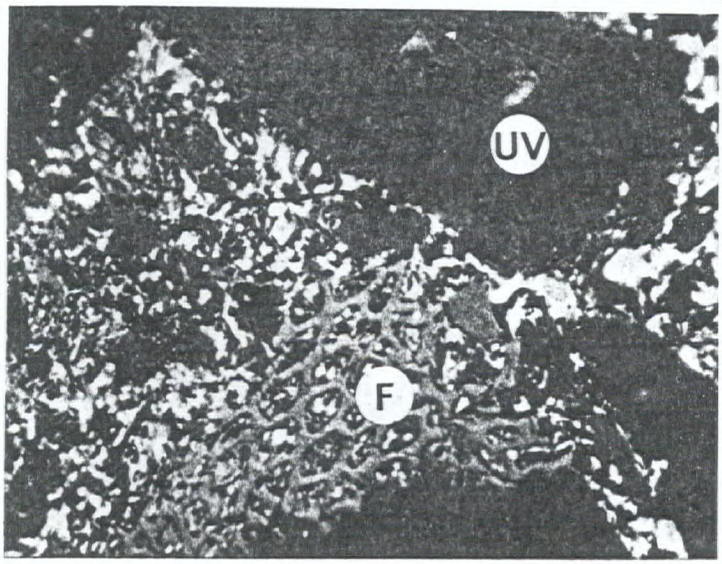

Fig. 7 - Microstructure of the dilatation residue from hydrogenated Forestburg coal U.V. - unreacted vitrinite, F - Fusinite.

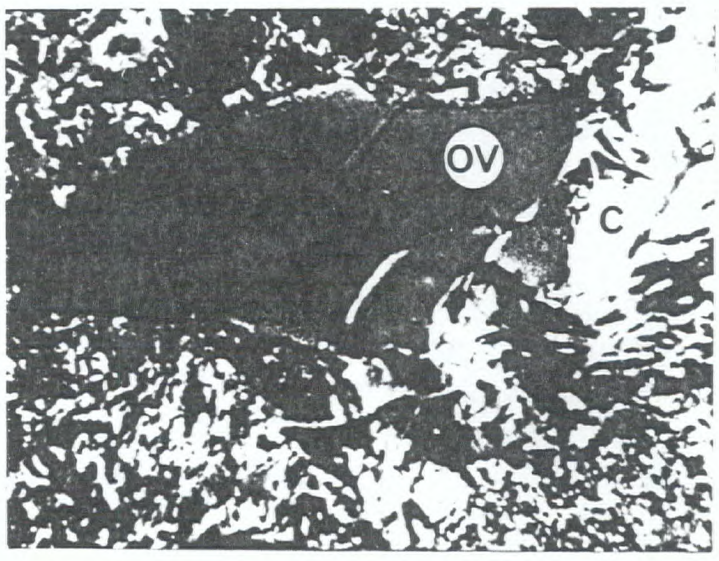

Fig. 8 - Micrograph of the dilatation residue from the hydrogenated product of oxidized Phalen Seam coal; O.V. - oxidized vitrinite C - Coke formation.

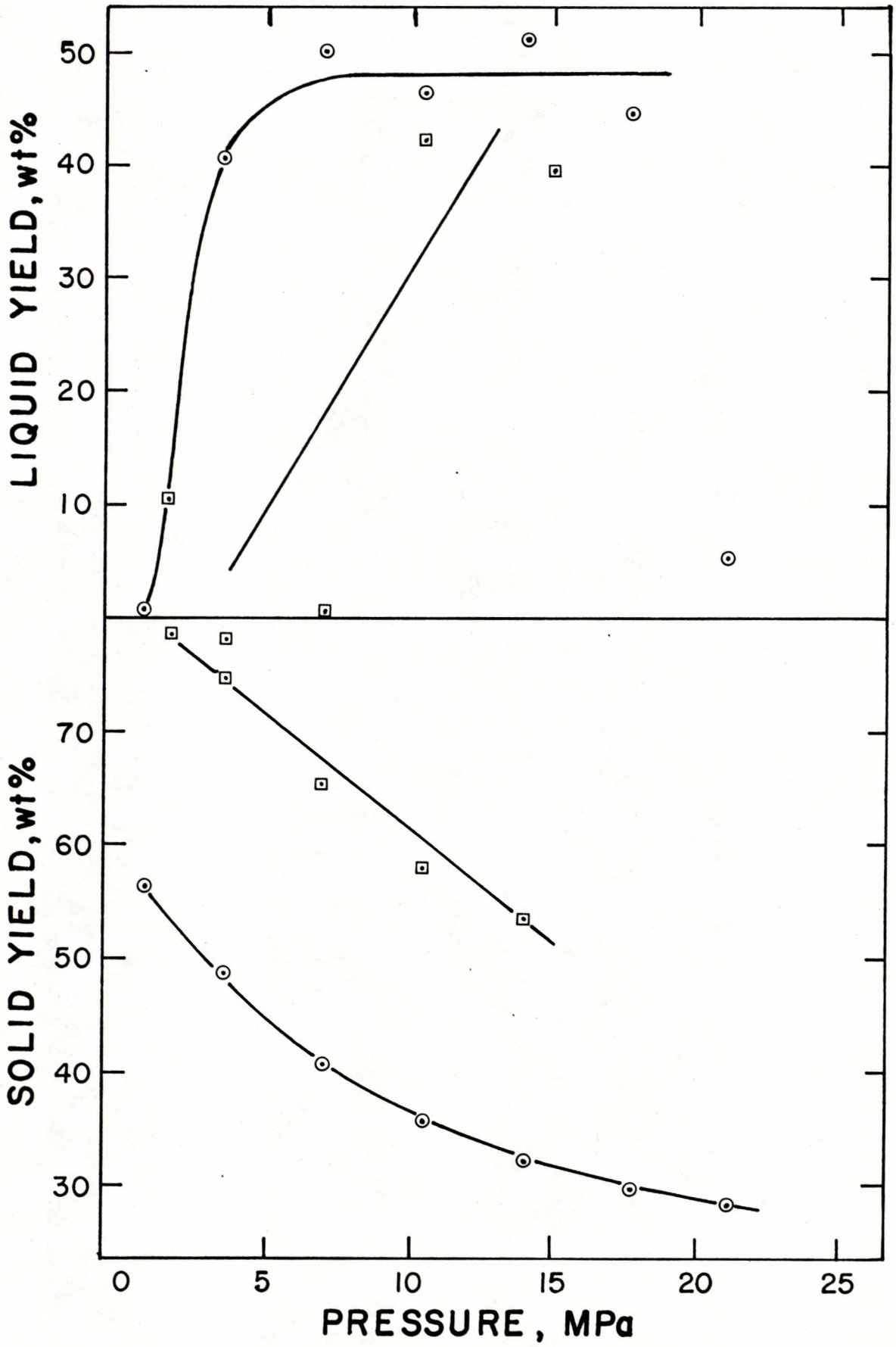

FIGURE 9 (NANDI JESUDASAN AND BLANCO)

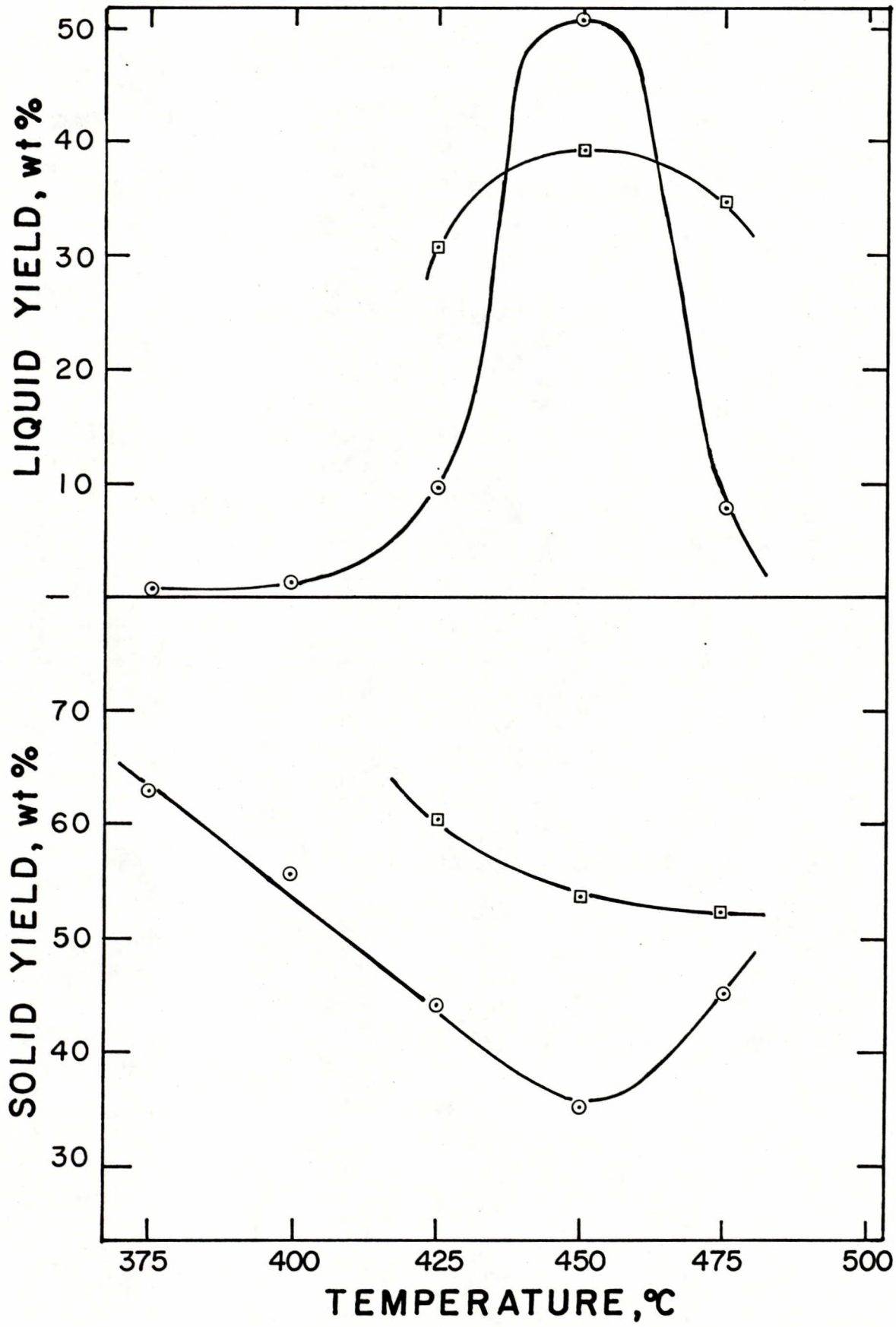

FIGURE 10 NAPHTHA TEMPERATURE AND PRESSURE

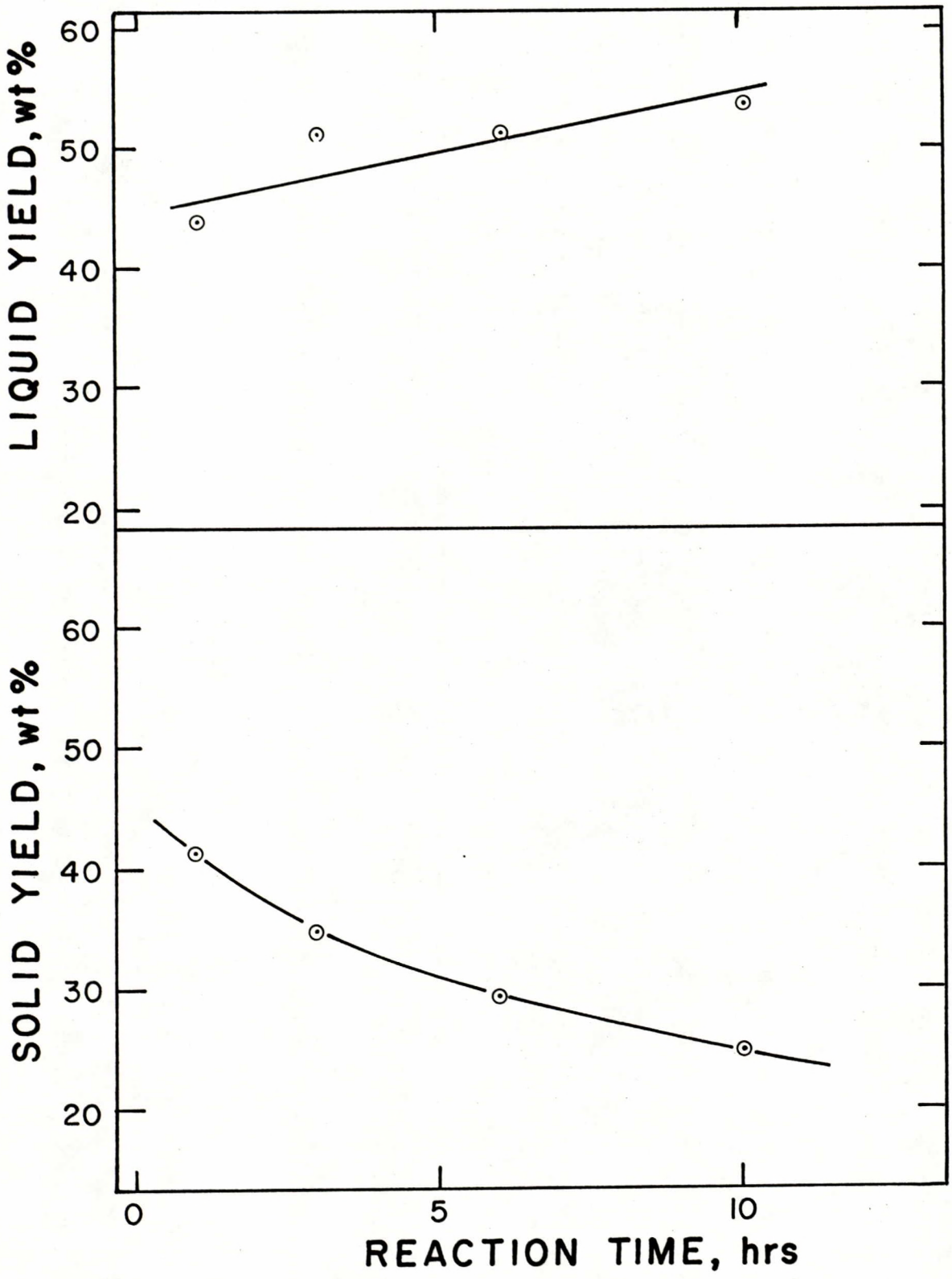

FIGURE 11 NANDI TERNIAN AND P. SUNKO

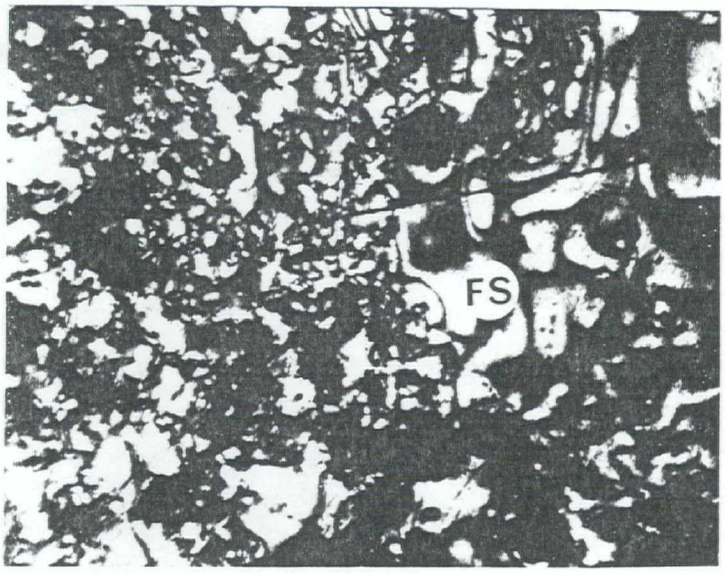

Fig. 12 - Dilatation residue of Forestburg coal after hydrogenation at 450°C and 13.9 MPa for 3 h, showing flow structure (F.S.).

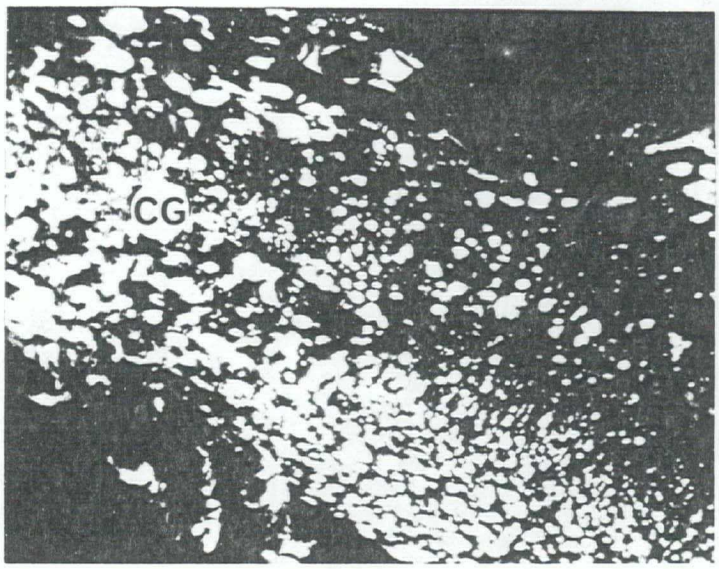

Fig. 13 - Dilatation residue of Forestburg coal after hydrogenation at 450°C and 6.9 MPa for 3 h, showing coarse grain structure (C.G.).

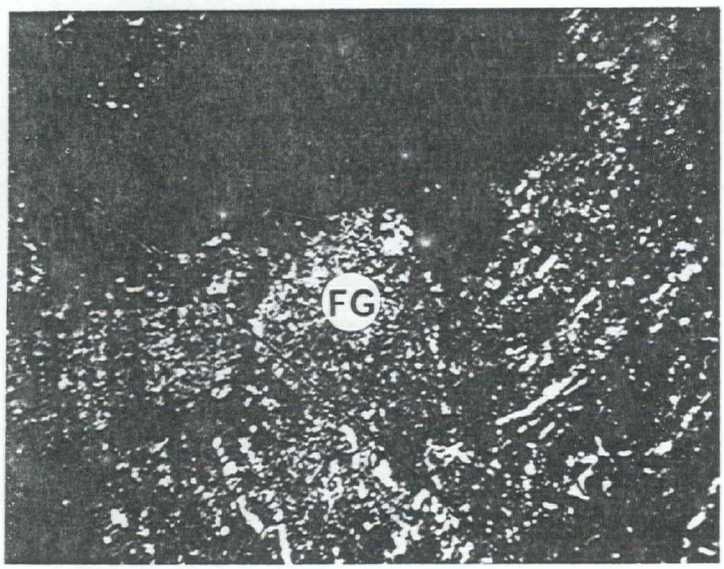

Fig. 14 - Dilatation residue of Forestburg coal after hydrogenation at 450°C and 3.5 MPa for 3 h, showing fine grain structure (F.G.).

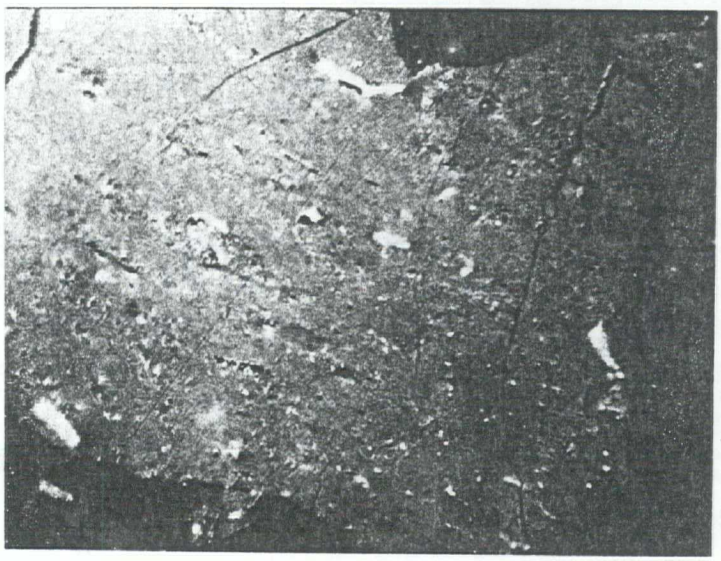

Fig. 15 - Dilatation residue of Forestburg coal after hydrogenation at 450°C and 0.79 MPa for 3 h, showing initial stage of fine grain structure.

Table 1 - Proximate and ultimate analyses of the coals used in these studies

		Onakawana lignite	Forestburg Sub-bituminous	Oxidized Phalen Seam bituminous	Canmore Semi-anthracite
Moisture	%	48.1	17.2	2.4	0.8
Ash	%	6.8	10.7	7.6	7.8
Volatile matter	%	21.4	31.1	32.2	13.4
Fixed carbon	%	23.7	41.0	57.8	78.0
Carbon	%	60.4	64.8	79.2	84.2
Hydrogen	%	3.9	4.0	5.0	3.7

Table 2 - Dilatation properties of the original coals

	Onakawana lignite	Forestburg Sub-bituminous	Oxidized Phalen Seam bituminous	Canmore Semi-anthracite
Softening temperature θ_s °C	< 310	343	339	499
Maximum contraction C %	8	10	20	2
Temp. of max. contr. θ_c °C	478	483	446	550
Maximum dilatation %	Nil	Nil	Nil	Nil
Temp. of max. dil. °C	Nil	Nil	Nil	Nil
Plasticity index $C/(\theta_c - \theta_s)$	-	0.07	0.19	0.04
F.S.I.	NA	NA	3	NA

NA = non-agglomerating

Table 3 - Dilatation properties of coals after hydrogenation at 450°C, 13.9 MPa, 3.0 h

	Onakawana lignite	Forestburg Sub-bituminous	Oxidized Phalen Seam bituminous	Canmore Semi-anthracite
Softening temperature θ_s °C	< 300	233*	< 290*	412
Maximum contraction C %	11	16	16	2
Temp. of max. contr. θ_c °C	331	312	362	475
Maximum dilatation %	6	175	50	Nil
Temp. of max. dil. °C	414	472	464	Nil
Plasticity index $C/(\theta_c - \theta_s)$	-	0.20	-	0.03
F.S.I.	$1\frac{1}{2}$	$2\frac{1}{2}$	$5\frac{1}{2}$	5

*Standard test modified for low softening temperature

Table 4 - Dilatation properties of coals after thermal treatment in nitrogen at 450°C, 13.9 MPa, 3.0 h

	Onakawana lignite	Forestburg Sub-bituminous
Softening temperature θ_s °C	N.S.	N.S.
Maximum contraction C %	Nil	Nil
Temp. of max. contr. θ_c °C	Nil	Nil
Maximum dilatation %	Nil	Nil
Temp. of max. dil. °C	Nil	Nil
Plasticity index $C/(\theta_c - \theta_s)$	-	-
F.S.I.	N.A.	N.A.

N.S. - No softening

N.A. - Non-agglomerated

Table 5 - Effect of gas pressure on dilatation properties of Forestburg coal after hydrogenation at 450°C for 3 h

Pressure MPa	0.79	3.5	7.0	10.4	13.9
Softening temperature θ_s °C	Nil	Nil	347	273*	233*
Maximum contraction C %	Nil	Nil	2	3	16
Temp. of max. contr. θ_c °C	Nil	Nil	441	387	312
Maximum dilatation %	Nil	Nil	Nil	Nil	175
Temp. of max. dil. °C	Nil	Nil	Nil	Nil	472
Plasticity index $C/(\theta_c - \theta_s)$	Nil	Nil	0.02	0.03	0.20

*Standard test modified for low softening temperature coal

Table 6 - Effect of temperature on dilatation properties of Forestburg coal after hydrogenation at 13.9 MPa for 3 h

Temperature °C	375	400	425	450	475	500
Softening temperature θ_s °C	414	448	335	233*	312	428
Maximum contraction C %	2	2	7	16	20	3
Temp. of max. contr. θ_c °C	478	503	498	312	394	493
Maximum dilatation %	Nil	Nil	Nil	175	39	Nil
Temp. of max. dil. °C	Nil	Nil	Nil	472	475	Nil
Plasticity index $C/(\theta_c - \theta_s)$	0.03	0.04	0.04	0.20	0.24	0.04

*Standard test modified for low softening temperature coal

Table 7 - Effect of reaction time on dilatation properties of Forestburg coal after hydrogenation at 450°C and 13.9 MPa

Reaction time h	0	1	3	6	10
Softening temperature θ_s °C	NS	350	233*	319	322
Maximum contraction C %	Nil	11	16	17	17
Temp. of max. contr. θ_c °C	Nil	460	312	392	391
Maximum dilatation %	Nil	Nil	175	23	13
Temp. of max. dil. °C	Nil	Nil	472	477	477
Plasticity index $C/(\theta_c - \theta_s)$	-	0.10	0.20	0.23	0.24

*Standard test modified for low softening temperature coal

NS = No softening

Table 8 - Effect of gas pressure on dilatation properties of oxidized Phalen Seam coal after hydrogenation at 450°C for 3 h

Pressure MPa	1.5	3.5	7.0	10.4	13.9
Softening temperature θ_s °C	NS	NS	412	350	< 290
Maximum contraction C %	Nil	Nil	3	19	16
Temp. of max. contr. θ_c °C	Nil	Nil	366	415	-
Maximum dilatation %	Nil	Nil	Nil	5	50
Temp. of max. dil. °C	Nil	Nil	Nil	481	464
Plasticity index $C/(\theta_c - \theta_s)$	-	-	0.06	0.29	-

NS = No softening

Table 9 - Effect of gas pressure on oxygen content of oxidized Phalen Seam coal after hydrogenation at 450°C for 3 h

Pressure MPa	Oxygen wt %
1.4	6.6
3.5	6.2
6.9	3.7
13.9	2.5

Table 10 - Effect of reaction time on oxygen, nitrogen and sulphur content of Forestburg coal after hydrogenation at 450°C and 13.9 MPa

Reaction time hours	Oxygen wt %	Nitrogen wt %	Sulphur wt %
0	7.7	1.7	0.4
1	4.3	1.8	0.4
3	4.0	1.6	0.5
6	3.8	1.6	0.4
10	-	1.5	0.4